

1 • Article type: paper

2

3 Title

4

5 Is colour change a good measure of a water penetration front?

6

7

8 Author 1

9 • N. Fischer, engineering doctorate student

10 • HeidelbergCement Technology Center, Oberklamweg 6, 69181 Leimen,
11 Germany

12 • Micro and NanoMaterials and Technologies Industrial Doctorate Centre,
13 University of Surrey, Guildford, United Kingdom

14 Author 2

15 • R. Haerdtl, Dr-Ing.

16 • HeidelbergCement Technology Center, Oberklamweg 6, 69181 Leimen,
17 Germany

18 Author 3

19 • P. J. McDonald, Professor of Physics

20 • Department of Physics, University of Surrey, Guildford, Surrey, United
21 Kingdom

22

23

24 Corresponding author: P. J. McDonald, Department of Physics, University of
25 Surrey, Guildford, Surrey, GU2 7XH, United Kingdom p.mcdonald@surrey.ac.uk

26

27

28

29 Abstract

30 GARField nuclear magnetic resonance (NMR) profiling is used to
31 demonstrate that the sharp colour change boundary commonly used to locate
32 the water front in cement and concrete capillary absorption tests is a poor
33 indicator of the true depth of water penetration. Across a range of mortars and
34 concretes, NMR invariably shows a smooth and often near zero gradient in the
35 degree of saturation at this boundary. Any sharp front that does exist, as might
36 arise from a strong dependence of the effective diffusivity on concentration and a
37 multimodal pore size distribution on the nanoscale is always far beyond the
38 colour change line.

39

40 Keywords

41 Capillary absorption; NMR; Colour boundary;

42

43 List of notation

44 w/c water to cement ratio

45 r_K Kelvin-radius

46 ψ relative humidity

47 T temperature

48 M molar mass

49 σ surface tension

50 ρ density

51 θ contact angle between liquid and solid

52 R gas constant

53 T_2 nuclear spin-spin relaxation time

54

55 **1. Introduction**

56 Visual observation of a colour change at a water ingress front in
57 cementitious materials is a common method to determine water uptake in test
58 methods such as the sorptivity and the water penetration under pressure test
59 (BS EN 12390-8:2009).

60 Sorptivity is measured by capillary uptake and has units of distance per
61 root time: $m s^{-1/2}$. Sorptivity was first introduced by (Philip 1957) in the field of
62 hydrology. Hall (Hall 1977, Hall 1981) subsequently applied the term and test
63 procedure to cementitious materials. The test comprises of placing a pre-dried
64 sample above a water reservoir and watching the capillary uptake of water into
65 the porous structure. Either the increasing mass of the sample is measured at
66 intervals during the capillary uptake, or the sample is split and an internal
67 surface inspected for a visual water front. In the latter case, a plot of depth of
68 penetration against square root of time is expected to be a straight line for times
69 sufficiently short that the front does not approach the other end of the sample. It
70 has been noted before that the sorptivity derived from mass uptake and
71 penetration depth analyses usually differ (Basheer 2001). Moreover, in the case
72 of visual measurements, it has been suspected that some water ingresses beyond
73 the colour change front (Hall, Hoff 2009).

74 The water penetration under pressure test as a measure of permeability
75 was first introduced by (Murata 1965). Several mix designs, durations of test and
76 applied pressure were investigated. It was concluded that the water penetration
77 depth determined by visual observation was an appropriate method to measure
78 permeability. RILEM Recommendations (RILEM TC 1994) specified the area
79 where pressure is applied depending on sample size and also the applied
80 pressure steps and duration. The test procedure became standardised in
81 Germany in 1986 (DIN 1048:5 1991) and then used internationally (ISO/DIS
82 7031). These standards used a similar procedure to the technical
83 recommendation. The German standard later became the base for the current EN
84 12390-8 European standard.

85 The purpose of this short report is to present nuclear magnetic resonance
86 imaging (MRI) evidence that the colour change front can present a significantly

87 inaccurate measure of the actual water from position. Profiles of the water
88 concentration profile in mortar cylinders after 1 day of capillary absorption
89 obtained using a laboratory GARField NMR system (Glover et al. 1999) are
90 compared to photographic recording of the colour-change front. Data sets show
91 that the water penetrated region extends well beyond that indicated by visual
92 observation of the colour boundary. Parallel measurements using a Surface
93 Garfield NMR system (McDonald et al. 2007) of the water capillary absorption
94 profile into the surface of concrete blocks show similar effects. The temporal
95 development of the water concentration spatial profile, the water distribution
96 within the open porosity, and evidence for C-S-H swelling in the same materials
97 are reported elsewhere (Fischer et al 2014, Fischer 2014).

98

99 **2. Materials and Methods**

100

101 **2.1. Materials.**

102 Standard mortar(BS EN 196-1:2005) samples were mixed and cast into
103 cubic moulds of 150 mm side length. The mortar mix had a ratio of 0.5 : 1 : 3 by
104 mass for water : binder : aggregate. Two different binders were investigated,
105 Portland cement and Portland cement with 10 % silica fume by mass added at
106 mixing. One day after casting, the cubes were removed from the moulds and
107 further cured at 20°C for a minimum of 3 months either sealed in a double layer
108 of plastic sheet or underwater in lime water. One cube was prepared for each
109 mixture and curing method.

110 Cylinders of 18 mm diameter and 150 mm length were wet cored from
111 the cured cubes. The paste skin that forms on the surface of the sample at casting
112 was not removed from the end of the cylinders. The mortar cylinders were dried
113 to constant mass at 60°C, and under light vacuum to minimise carbonation, over
114 a period of about 2 weeks. After drying, the samples were wrapped with PTFE
115 tape with the two ends open.

116 The cylindrical samples were then exposed to liquid tap water from one
117 end. To do this, the cylinders were suspended above a shallow pool of water with

118 the lower end 1-2 mm below the water surface. The water level was kept
119 constant. The PTFE wrapping prevented drying from the sides and encouraged
120 one-dimensional water transport along the length of the cylinders. Other
121 common sealants and tapes, such as epoxy coating could not be used as they give
122 a significant ^1H background signal in NMR.

123 Concrete slabs were also investigated with the same binders and w/b
124 ratio. An example of a sealed cured OPC concrete and an OPC with 10% silica
125 fume are included in this report. The concrete slabs were cut from the centre of
126 the 150 mm cubes. Similarly to the mortars, the samples were dried to constant
127 mass at 60°C. After drying, the cut surface was stood in water for the uptake test.
128 The sides of the slabs where the colour-change water-front line was observed
129 had a thin paste skin originating from casting / curing. To ensure that this did
130 not significantly affect the results, a slab was split in half to observe the internal
131 water-front. It was found to be in good agreement with the surface.

132

133 **2.2. Methods**

134 Capillary water absorption was assessed in three ways: gravimetrically,
135 by observation (photographic recording) of the colour-change front and by ^1H
136 spatially localised NMR relaxometry. The sample mass was measured after 1, 2,
137 4, 8 and 24 hours of capillary absorption. The purpose was to ensure that we
138 remained in the region of linear dependence of uptake on the square root of
139 time. A photograph of the sample with the same reference white background and
140 scale was taken after 24 hours of capillary absorption. An NMR profile was also
141 acquired after 24 hours of capillary absorption. In general, more frequent
142 periodic recording was not done, as this would have required overly exposing
143 the sides of the sample to the atmosphere. For NMR profiling, mortar cylinders
144 were stepped through the resonant plane of a laboratory GARField magnet. The
145 step size was normally 1 mm. At each step, a Carl-Purcell-Meiboom-Gill (CPMG)
146 echo train was recorded (Meiboom, Gill 1958). The ^1H NMR frequency was 23.4
147 MHz and the $\pi/2$ pulse length was 6.5 μs . A total of 64 echoes with 64 μs echo
148 spacing and 2048 averages were recorded at each step.

149 A simple profile of the water content was constructed by summing the
150 echo intensities at each location. This yields a profile with a relatively good
151 signal-to-noise ratio. However, the echo-sum intensity is not linearly
152 proportional to water content. A better measure is provided by fitting the echo
153 train data to multi-exponential decays. It is well established that water in more
154 mobile environments / larger pores exhibits a longer decay time. To that end, the
155 first 2 echoes (that contain a significant contribution from the hydrate gel
156 interlayer water and that can suffer from artefact) were disregarded at each
157 location and the remainder fit to a two component exponential decay plus
158 baseline representing water in gel pores, interhydrate spaces and capillary pores
159 respectively (Muller et al 2013). The sum of these three amplitudes is thus a
160 measure of the evaporable water content. The baseline was used since the
161 maximum echo time (4.1 ms) was less than the expected decay time of capillary
162 water. Chemically combined water (in, e.g. Portlandite) has a decay time too
163 short for even the first echo.

164

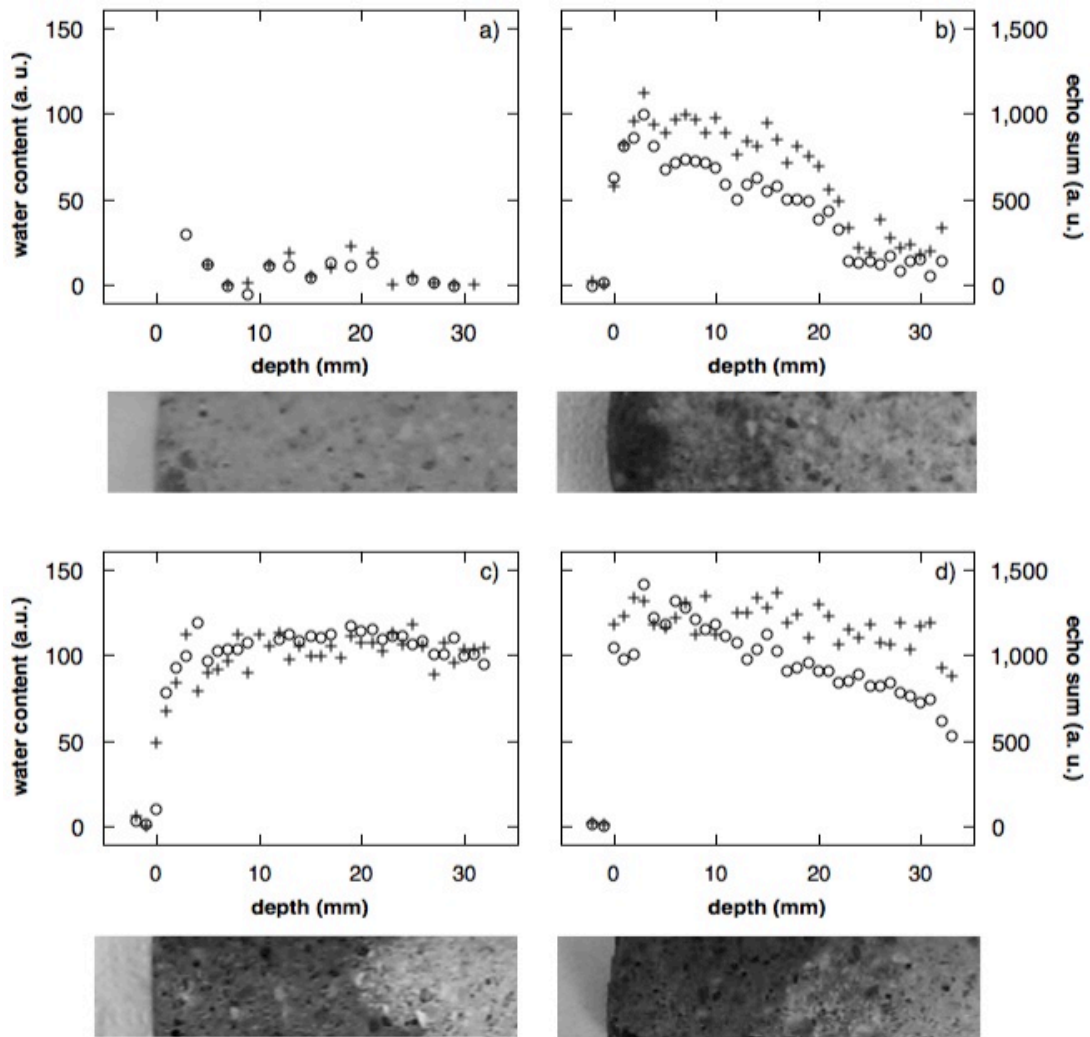
165 **3. Results and analysis**

166 Figure 1a and 1b show NMR profiles of water in the first 32 mm of sealed-
167 cured OPC-mortar cylinders after drying and again after 1 day of capillary
168 absorption respectively. The exposed surface is at 0 mm on the scale. The
169 profiles are constructed in two ways: as echo sum data (right hand access) and
170 from the total amplitude of the exponential fits to the echo train data (left hand
171 access). Typically for the parameters used most of the signal occurs in the first
172 10-12 echoes. Hence the echo sum is about ten times the initial amplitude,
173 though both are of course in arbitrary units. The profiles show water invading
174 about 22 mm into the sample, with a sharp front at about 22 mm on the scale.
175 The fact that the pre-absorption intensity is close to baseline supports the claim
176 that evaporable water is being monitored. According to the echo sum data, there
177 is a significant gradient in concentration across the invaded region after 1 day of
178 capillary absorption. However, this is much less evident in the intensity derived
179 from the echo-train fitting analysis. The difference likely reflects a redistribution

180 of the water in the nanoscale porosity due to C-S-H swelling that is discussed
181 elsewhere (Fischer et al 2014).

182 Photographs of the same section of the cylinder before and after capillary
183 absorption are shown immediately below the profile plots. The photographs are
184 all greyscale and slightly enhanced for brightness. All photographs were taken
185 with the same white background. Before capillary absorption, the dry sample is
186 uniformly light coloured. After 1 day of capillary absorption there is a clear
187 darkening of the wetted surface layers with a clear colour boundary at about 5
188 mm. Beyond this the sample is slightly darker and there is an indication a weaker
189 colour change at about 14 mm. However, whichever boundary is taken as the
190 water front, neither extends as far as the NMR shows water to penetrate.

191 Figure 1c and 1d repeat figure 1b for two further samples of the same
192 mortar. In these samples, the water travels much further in one day by both
193 measures. The visual interface is much more evident in these samples and so the
194 results are even less ambiguous. The NMR profile shows greater ingress than the
195 optical measurement in each case. Indeed, in the case of 1b water extends
196 beyond 32 mm. The water concentration measured by NMR is relatively smooth
197 across the visual interface. However, careful observation suggests that there is a
198 slight change in gradient at the colour change, notably for the echo sum data.
199 Echo sum has the effect of magnifying the contribution of water content in larger
200 capillary pores relative to smaller gel pores. A key question is why the capillary
201 absorption in figure 1b is substantially less than in figure 1c or 1d. The answer
202 lies in the sample history. The sample used for figure 1b was cast in May, cured
203 sealed, cored and dried in August and used for capillary absorption in January.
204 Those for figures 1c and 1d were cast in May (same cube) cored and dried in
205 January and used for capillary absorption in February.

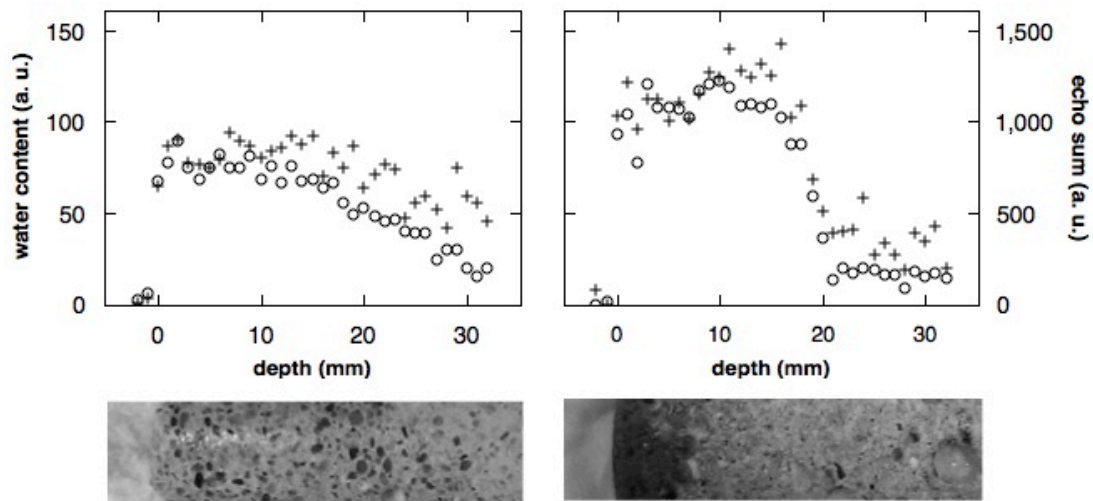


206

207 Fig 1. NMR profiles and photographs of a sealed cured OPC mortar
 208 cylinder use in capillary absorption experiments: (a) dry and (b) after 1 day of
 209 capillary absorption. The profiles are constructed from echo sums (circles, right
 210 hand axes) and exponential fitting intensities (crosses, left hand axes). (c) and
 211 (d) are profiles and photographs of 2 further samples after 1 day of capillary
 212 absorption. All cylinders were cored from the same cube of mortar. The cylinder
 213 used in (a and b) was dried 4 months before use. The cylinders in (c and d) were
 214 not dried until needed.

215 Figure 2 shows examples of an underwater cured OPC mortar and a
 216 sealed cured OPC mortar with silica fume after 1 day of capillary absorption. In
 217 case of the underwater cured sample, the wet region is less marked in the
 218 photographs. Notwithstanding, a weak colour change boundary can be discerned

219 at about 22 mm on the scale. The NMR profile constructed from the echo sum
 220 shows a gradual water concentration gradient right across this boundary. The
 221 profile constructed from the fitted echo amplitude is more constant around 22
 222 mm with a more marked interface nearer 30 mm. In the case of the sample with
 223 silica fume, the water front is much more marked, both optically and by NMR.
 224 However, the former is at about 6 mm depth, whereas the latter is at about 18
 225 mm.

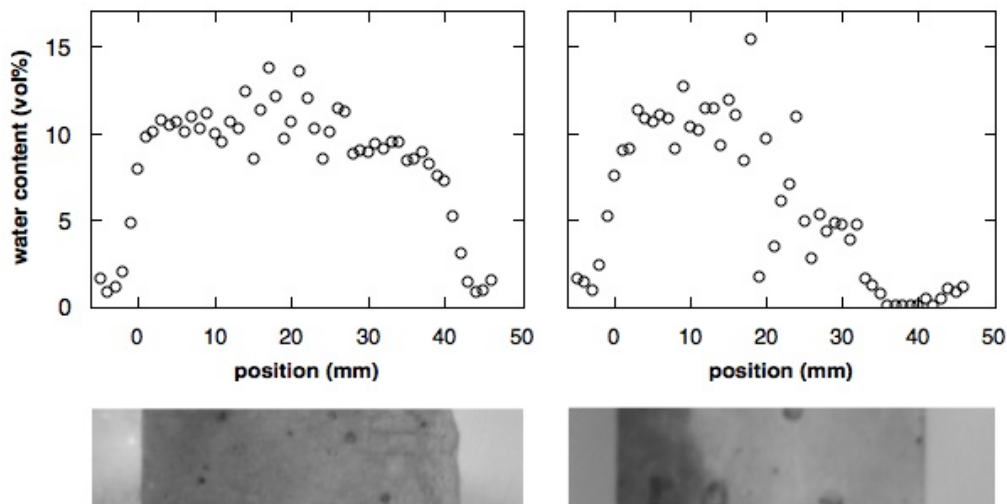


226
 227 Fig 2. Under water cured OPC mortar (left) and sealed cured OPC with
 228 silica fume mortar (right) sample after 1 day of capillary absorption. NMR profile
 229 of gel+capillary water (crosses, left axes) and echo sum (circles, right axes).
 230 Photographs of the same area are below the NMR data

231
 232 In total, 4 sealed and 2 underwater cured OPC mortars and 3 sealed cured
 233 OPC mortars with silica fume were investigated. In every case the water ingress
 234 as measured by NMR profiling extended significantly beyond the water front
 235 indicated by the colour change boundary. In no case, was there an unambiguous
 236 sharp feature in the NMR data at the colour change boundary.

237
 238 Figure 3 shows two concrete samples measured by the surface GARField.
 239 The signal to noise ratio decreases with depth with surface GARField. The

240 profiles shown are constructed from measurements from both sides of the
241 sample. Hence the signal to noise ratio of the data is worst in the profile centre.
242 The profiles are shown as echo sums only as the signal to noise ratio in these
243 measurements did not permit exponential fitting. The surface in contact with
244 water is at 0 mm. The photographs of the cross section of the samples are below
245 the NMR profiles. In case of the OPC concrete, the sample was wet all the way
246 through as measured by NMR. However, the photograph shows a gradual colour
247 change boundary nearer 15 mm. The first 15 mm from the left side is darker
248 than the rest of the sample. In the case of the OPC concrete with silica fume there
249 is an even more clear water line, about 10 mm from the wet surface. However,
250 the NMR profile shows water extending well beyond this dark region, down to
251 about 30 mm from the wet surface.



252

253 Fig 3. Echo sum NMR profiles concrete samples after 1 day of capillary
254 absorption with photographic cross-sections below. The samples are sealed
255 cured OPC concrete (left) and OPC concrete with silica fume (right).

256

257 4. Discussion

258 In a capillary uptake experiment, there is a gradient of internal relative humidity
259 in the sample from 100% where the sample is in contact with liquid water down
260 to the ambient value at the exposed end. Capillary uptake of water at the lower

261 end, evaporation at the water front, and a detailed liquid and vapour mass flow
262 rate balance through pore network lead to a non-uniform water content profile as
263 has been discussed by Hall and Hoff (Hall, Hoff 2009).

264 Theoretical understanding of the colour change of wetted porous ceramic bricks
265 has been discussed previously (Hall, Hoff 2009). It is a complex problem. Not
266 withstanding, it is reasonable to assume that the colour change is associated with
267 the wetting of pores of size comparable to the wavelength of light, circa 400-700
268 nm. The Kelvin equation

$$r_K = -\frac{2\sigma M \cos \theta}{RT\rho \ln \psi}$$

269 gives the critical radius, r_K , of a pore that is filled with water at a relative
270 humidity, ψ , and temperature, T . In this equation M is the molar mass, σ the
271 surface tension, ρ the density and θ the contact angle of the liquid in the pore and
272 R is the gas constant. For optical wavelengths, and using parameters for water
273 and assuming that water wets cement, this suggests that the colour change
274 occurs at relative humidities exceeding 99.7 %.

275 The NMR signal lifetime, (the nuclear spin-spin relaxation time, T_2) of ^1H in
276 water in small pores is proportional to the pore size (D'Orazio et al. 1990). The
277 NMR measurements made in this work are sensitive to water in gel pores (a few
278 nanometres), inter-hydrate pores (a few tens of nm) and larger capillary pores
279 (100 nm to mm) resultant from chemical shrinkage and air voids in the original
280 mix (Muller et al. 2013). By the Kelvin equation, and taking representative sizes
281 of 3, 30, 300 and 3000 nm, these different pore sizes fill at relative humidities of
282 70, 96, 99.6% and >99.9%. There is inevitably a (non-constant) gradient in
283 vapour pressure across the sample during capillary absorption: the upper face of
284 the sample is in equilibrium with the atmosphere. Given that the NMR senses
285 water across a very wide range of pore sizes, and hence relative humidities, it is
286 therefore reasonable to expect that water is seen over a great spatial range. One
287 does not then expect to see a sharp feature in the NMR water profile at the colour
288 change boundary. Such sharp boundaries as do occur are beyond this line and
289 could well be associated with the multi-modal pore size distribution on the nano-
290 scale as revealed by NMR (Muller et al. 2013).

291

292 **5. Conclusions**

293 A colour change boundary line is often used to determine the penetration
294 waterfront in cement and concrete water transport test procedures. The results
295 should be treated with caution. NMR profiling yields clear evidence that there is
296 significant amount of water beyond the colour change line in capillary
297 absorption tests. In most cases, the degree of saturation of the sample is only
298 marginally less beyond the darkened region and there is, in general, no marked
299 change in the degree of saturation gradient as this boundary is crossed.
300 Notwithstanding, in many instances there is a sharp water front as predicted by
301 several numerical models on the basis of a strong dependence of the effective
302 diffusivity on pore size and vapour pressure and hence saturation. However, as
303 shown by NMR, it occurs significantly beyond the optical boundary.

304 The results in this paper focused on water ingress into dried material. The
305 water penetration under pressure test focuses on water ingress into already wet
306 material. This test also relies on visual observation. Other experiments to be
307 reported elsewhere (Fischer 2014) show that NMR does not detect a strong front
308 under those conditions either.

309

310 **Acknowledgements**

311 The research leading to these results has received funding from the
312 European Union Seventh Framework Programme (FP7/2007-2013) under grant
313 agreement 264448

314

315 **References**

- 316 Basheer, P.A.M. 2001, "16 - Permeation Analysis" in *Handbook of Analytical*
317 *Techniques in Concrete Science and Technology*, eds. V.S. Ramachandran & J.J.
318 Beaudoin, William Andrew Publishing, Norwich, NY, pp. 658-737.
- 319 BS EN 12390-8:2009 *Testing hardened concrete - Part 8: Depth of penetration of*
320 *water under pressure.*

- 321 BS EN 196-1:2005 *Methods of testing cement. Determination of strength.*
- 322 DIN 1048:5 1991, *Prüfverfahren für Beton; Festbeton, gesonderd hergestellte*
323 *Probekörper.*
- 324 D'Orazio, F., Bhattacharja, S., Halperin, W.P., Eguchi, K. & Mizusaki, T. 1990,
325 "Molecular diffusion and nuclear-magnetic-resonance relaxation of water in
326 unsaturated porous silica glass", *Physical Review B*, vol. 42, no. 16, pp. 9810-
327 9818.
- 328 Fischer, N. 2014, *Validation of conventional water transport test methods by*
329 *spatially resolved ¹H magnetic resonance*, EngD thesis, University of Surrey,
330 (in preparation).
- 331 Fischer, N., Haerdtl, R. & McDonald, P.J. 2014, "Observation of the redistribution
332 of nanoscale water filled porosity in cement based materials during wetting"
333 *Cement and Concrete Research* (submitted)
- 334 Glover, P. M., Aptaker, P.S., Bowler J.R., Ciampi, E. and McDonald P.J., 1999 "A
335 novel high gradient permanent magnet for the imaging of planar thin films",
336 *Journal of Magnetic Resonance*. vol. 139, no 1, pp. 90-97.
- 337 Hall, C. & Hoff, W.D. 2009, *Water Transport in Brick, Stone, and Concrete*, 2nd edn,
338 Spon Press.
- 339 Hall, C. 1981, "Water movement in porous building materials—IV. The initial
340 surface absorption and the sorptivity", *Building and Environment*, vol. 16, no.
341 3, pp. 201-207.
- 342 Hall, C. 1977, "Water movement in porous building materials—I. Unsaturated
343 flow theory and its applications", *Building and Environment*, vol. 12, no. 2,
344 pp. 117-125.
- 345 ISO/DIS 7031 "Concrete hardened - Determination of the depth of penetration of
346 water under pressure", .
- 347 McDonald, P.J., Aptaker, P.S., Mitchell, J. & Mulheron, M. 2007, "A unilateral NMR
348 magnet for sub-structure analysis in the built environment: The Surface
349 GARField", *Journal of Magnetic Resonance*, vol. 185, no. 1, pp. 1-11.
- 350 Meiboom, S. & Gill, D. 1958, "Modified spin-echo method for measuring nuclear
351 relaxation times", *Review of Scientific Instruments*, vol. 29, no. 8, pp. 688-691.
- 352 Muller, A.C.A., Scrivener, K.L., Gajewicz, A.M. & McDonald, P.J. 2013,
353 "Densification of C-S-H Measured by ¹H NMR Relaxometry", *The Journal of*
354 *Physical Chemistry C*, vol. 117, no. 1, pp. 403-412.
- 355 Murata, J. 1965, "Studies on the Permeability of Concrete", *Materials and*
356 *Structures*, , no. 29, pp. 47-54.

- 357 Philip, J.R. 1957, "The Theory of Infiltration: 4. Soprtivity and Algebraic
358 Infiltration Equations", *Soil Science*, vol. 84, no. 3, pp. 257-264.
- 359 RILEM TC 1994, "CPC 13.1 Teste for the penetration of water under pressure on
360 hardened concrete, 1979" in *RILEM Recommendation for the Testing and Use
361 of Construction Materials*, ed. RILEM, E & FN SPON, , pp. 41-42.
- 362